Pöyhönen, Kim; Ojanen, Teemu

Superlattice platform for chiral superconductivity with tunable and high Chern numbers

Published in:
Physical Review B

DOI:
10.1103/PhysRevB.96.174521

Published: 27/11/2017

Document Version
Publisher's PDF, also known as Version of record

Please cite the original version:
Pöyhönen, K., & Ojanen, T. (2017). Superlattice platform for chiral superconductivity with tunable and high Chern numbers. *Physical Review B*, *96*(17), 1-5. Article 174521. https://doi.org/10.1103/PhysRevB.96.174521

Superlattice platform for chiral superconductivity with tunable and high Chern numbers

Kim Pöyhönen and Teemu Ojanen
Department of Applied Physics (LTL), Aalto University, P. O. Box 15100, FI-00076 AALTO, Finland
(Received 14 September 2017; published 27 November 2017)

Finding concrete realizations for topologically nontrivial chiral superconductivity has been a long-standing goal in quantum matter research. Here, we propose a route to a systematic realization of chiral superconductivity with nonzero Chern numbers. This goal can be achieved in a nanomagnet lattice deposited on top of a spin-orbit coupled two-dimensional electron gas (2DEG) with proximity s-wave superconductivity. The proposed structure can be regarded as a universal platform for chiral superconductivity supporting a large variety of topological phases. The topological state of the system can be electrically controlled by, for example, tuning the density of the 2DEG.

DOI: 10.1103/PhysRevB.96.174521

I. INTRODUCTION

The Bardeen-Cooper-Schrieffer (BCS) theory explains superconductivity in terms of paired electrons, Cooper pairs, that condense in the same quantum state with a macroscopic population. One of the most striking subsequent predictions was the fact that a condensate could carry net angular momentum, giving rise to macroscopic chirality. However, candidates for chiral superconductors are rare [1]. From the modern point of view, two-dimensional (2D) chiral superconductors are naturally discussed in the context of topologically nontrivial states of matter that are classified by the Chern number invariant [2–4]. In intrinsic chiral superconductors, the Chern number is fixed to a certain value determined by the microscopic form of interparticle interactions.

In this work, we introduce a universal platform for 2D topological superconductivity that realizes a large collection of states with distinct Chern numbers. The central elements of the studied system are a nanomagnet lattice deposited on two-dimensional electron gas (2DEG) with significant spin-orbit coupling which is made superconducting through the proximity effect. Importantly, fabrication of the studied system is within the reach of current technology. Furthermore, this system is tunable through structural design as well as by gate operation, which allows switching between the different topological states after the structure is fixed.

The proposed nanomagnet structure generalizes conceptually and operationally the ferromagnet-2DEG-superconductor sandwich structure that was proposed as a realization of the chiral state with Chern number one [5]. Instead of the simplest nontrivial state, our model exhibits a large number of distinct phases with multiple chiral Majorana edge states. The flexible tunability also enables edge-mode engineering through fabrication of topological phase boundaries in the system. Therefore, the studied system could serve as an ideal test bed for the Majorana edge modes. Motivated by studies of topological superconductivity in magnetic chains [6–16], 2D superconductors with large Chern numbers were previously discovered in superconducting surfaces decorated by magnetic atoms [17–19]. The long-range hybridization of subgap Yu-Shiba-Rusinov states [20–24] generally gives rise to rich, mosaiclike topological phase diagrams [17,18]. However, as a crucial difference to atomic systems, the presently studied system allows a high level of control in the fabrication, tuning, and operating the system.

In this paper, we solve the subgap spectrum of a circular magnet on a superconducting 2DEG system. The magnetic lattice problem is then formulated in terms of the subgap states of individual nanomagnets. Then, we solve the spectrum of one-dimensional (1D) and 2D magnetic lattices and investigate their topological properties. In the 2D case we discover a remarkably rich topological phase diagram, where the energy gaps protecting the states can be a significant fraction of the induced gap in the 2DEG. Our results indicate that the studied system offers an unprecedented opportunity to systematically probe chiral superconductivity in experimentally feasible systems.

II. SYSTEM

We consider a 2DEG proximity coupled to an s-wave superconductor. In addition, a collection of nanomagnets have been placed on top of this substrate as shown in Fig. 1. The precise lattice geometry of the nanomagnet arrangement is not important for the derivation of the general description. In the standard Nambu basis $\Psi = (\psi_\uparrow, \psi_\downarrow, \psi_\downarrow^\dagger, -\psi_\uparrow^\dagger)^T$, this system can be described by the 4×4 Bogoliubov–de Gennes Hamiltonian $H = H_0 + H_{\rm imp}(\mathbf{r})$, where

$$H_0 = \xi_k \tau_z + \alpha_R \mathbf{k} \times \boldsymbol{\sigma} \tau_z + \Delta \tau_x, \qquad H_{\rm imp}(\mathbf{r}) = \sum_j V_j(\mathbf{r} - \mathbf{r}_j). \tag{1}$$

Here, $\xi_k = \frac{k^2}{2m} - \mu$ is the kinetic energy, α_R the Rashba spin-orbit coupling, and Δ the induced superconducting order parameter. The matrices τ_i and σ_i act in particle hole and spin space, respectively. The magnets are assumed be in a direct

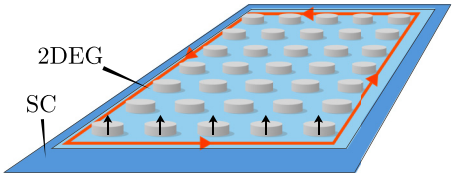

FIG. 1. An array of nanomagnets on a 2DEG substrate with spin-orbit coupling and proximity superconductivity realizes a highly tunable platform of topological superconductivity with a large number of nontrivial states.

contact with the 2DEG, inducing a perpendicular Zeeman potential $V_j(\mathbf{r})$, which takes the form

$$V_j(\mathbf{r}) = M_j\sigma_z\theta(R_j - |\mathbf{r}|). \tag{2}$$

This corresponds to homogeneous circular magnets, each with a radius R_i and magnetization energy scale M_i. In general, the magnets will also give rise to a local scalar potential. Since this effect only renormalizes the magnetic subgap states studied below, we will only consider the Zeeman part of the potential.

In analogy to the Yu-Shiba-Rusinov states of magnetic atoms on a superconductor, a single nanomagnet gives rise to energy states penetrating in the gap [24]. Similarly to magnetic atom chains [13], the topological properties of the nanomagnet lattice can be understood in terms of the subgap energy bands of hybridized bound states. We now wish to obtain an equation from which the energy bands and topological properties of the system can be discerned. From the equation $H\Psi = E\Psi$, by separating the magnetic potential on one side, we obtain the equation

$$\psi(\mathbf{k}) = \sum_j G_0(\mathbf{k},E)\int \frac{d^2q}{(2\pi)^2} e^{-i(\mathbf{k}-\mathbf{q})\cdot\mathbf{r}_j} V_j(\mathbf{k}-\mathbf{q})\psi(\mathbf{q}), \tag{3}$$

where $G_0(\mathbf{k},E) = (E - H_0)^{-1}$. The dependence here on two momenta makes an exact solution challenging. To simplify the problem, we follow the method of Refs. [25,26] and proceed by assuming that the potential terms $V_j(\mathbf{r} - \mathbf{r}_j)$, while having some finite spatial extent, are nevertheless radially symmetric about the point r_j, and that their Fourier transforms only weakly depend on the magnitude of the momenta $\mathbf{k},\mathbf{q}$. This allows us to expand the equation above in angular channels. For this reason, we introduce the quantities

$$\psi_i(\theta) \equiv \int \frac{k\,dk}{2\pi} e^{i\mathbf{k}\cdot\mathbf{r}_i}\psi(\mathbf{k}),$$

$$G_{ij}(E,\theta) \equiv \int \frac{k\,dk}{2\pi} e^{i\mathbf{k}\cdot(\mathbf{r}_i-\mathbf{r}_j)} G_0(E,\mathbf{k}),$$

which yield the angular momentum components through the integrals $G^l_{ij}(E) = \int \frac{d\theta}{2\pi} G_{ij}(E,\theta)e^{-il\theta}$ and $\psi^l_i(E) = \int \frac{d\theta}{2\pi}\psi_i(E,\theta)e^{-il\theta}$. The spectral problem then takes the form

$$\psi^l_i = \sum_j \sum_{l'} G^{l-l'}_{ij}(E) V_{j,l'}\psi^{l'}_j, \tag{4}$$

where the indices l,l' label the angular momentum components and i,j refer to the position indices of the nanomagnets. To solve the spectral problem (4), we must obtain expressions for the angular momentum components of the Green's function as well as the magnetic field. This derivation is done in the Supplemental Material (SM) [27], where the explicit forms of the results are also to be found. As shown there, the angular momentum components of the magnetic field are

$$V_{j,l} = 2\eta_j\sigma_z F_{j,l}/m, \tag{5}$$

where $\eta_j = M_j\pi m R^2/\hbar^2$ is a coupling term and $F_{j,l}$ is given in terms of Bessel functions in the SM. As $|l| \to \infty$, for a fixed radius R the terms F_l vanish as $\propto l^{-(2l+1)}$, and hence above some $|l| > l_{\max}$ we can approximate $F_l = 0$. This effectively reduces the infinite number of equations to a finite one, and it is then straightforward to write Eq. (4) as the nonlinear matrix eigenvalue problem

$$\left[\beta^2\begin{pmatrix} A & 0 \\ 0 & 0\end{pmatrix} + \beta\begin{pmatrix} V^{-1} & B \\ B & V^{-1}\end{pmatrix} - \begin{pmatrix} 0 & 0 \\ 0 & A\end{pmatrix}\right]\Psi = 0, \tag{6}$$

where $\beta = (\Delta + E)/\sqrt{\Delta^2 - E^2}$. In the above, A and B are $4(2l_{\max}+1)\times 4(2l_{\max}+1)$ matrices with submatrix elements A,B constructed from the Green's function, as detailed in the SM, and V is a diagonal matrix constructed from $V_{j,l}$. One can regard Eq. (6) as a tight-binding problem for eigenvalues E and eigenvectors Ψ. In contrast to ordinary tight-binding problems with a linear dependence on E, the energy dependence of the matrices in Eq. (6) is explicitly nonlinear. To work around this problem, previous works have mainly focused on the mid-gap regime where the system can be linearized in E. This also allows one to derive an effective Hamiltonian and solve a normal linear eigenvalue problem [13,26]. Since the linear approximation would force us away from the physically most interesting parameter regime of large energy gaps and robust topological states, we will employ methods to treat the full nonlinear problem [28,29]. We note again that Eq. (6) is in principle valid for any configuration of radially symmetric magnets, and does not assume that they are placed in some particular lattice.

III. SINGLE-MAGNET PROBLEM

We first consider the case where a single magnet rests on the substrate. This reduces the matrix in the nonlinear eigenvalue problem to be diagonal in indices i,j. By taking the determinant of the matrix to be zero, we can find the solution for an *arbitrary* value of $l_{\max}$ [27]. In terms of β, the eigenvalues obtained are

$$\beta_l = \begin{cases} \frac{\eta}{2}|F_l - F_{|l+1|} \pm \sqrt{(F_l - F_{|l+1|})^2 + \frac{4}{1+\varsigma^2}F_l F_{|l+1|}}\,|, & 0 \leqslant |l| < l_{\max} \\ \eta|F_l|, & |l| = l_{\max} \end{cases} \tag{7}$$

where $\varsigma = \alpha_R/v_F$. The bound-state energies are then obtained by using the relation $E_l = \Delta(\beta_l^2 - 1)/(\beta_l^2 + 1)$. Essentially, this constitutes a full solution of the bound-state energies; the expressions for $|l| < l_{\max}$ do not depend on the cutoff, and so it can safely be taken to infinity. Note that as $\beta_l \underset{l\to\infty}{\longrightarrow} 0$, we have $E_l \underset{l\to\infty}{\longrightarrow} \Delta$, so beyond a certain l the energies are effectively gapped out.

For the purposes of engineering a gapped topological superconductor, a large number of gap-filling bound states presents a problem. The way of counteracting this would be making the nanomagnets sufficiently small that the lowest-energy states are well separated from the rest, if possible. The parameter controlling the number of relevant bound states is $k_F R$, where k_F is the Fermi wave number of the 2DEG

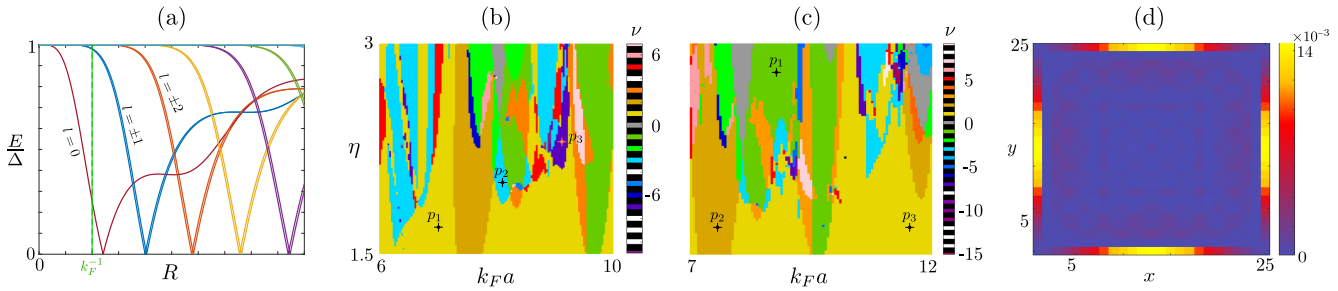

FIG. 2. (a) Bound-state energies as a function of radius R of a single magnet with constant magnetization. As $R \to 0$, the magnetic coupling vanishes, lifting the bound states to the gap. At $k_F R = 1$, all but the lowest three states are essentially gapped out. Parameters used are $\eta = 2$, $\varsigma = 0.1$ (b) Chern number diagram calculated in real space for a 17×17 system with $\xi/a = 2.5$, $R/a = 0.125$, $\varsigma = \alpha_R/v_F = 0.3$. The angular momentum cutoff is set at $l_{\max} = 1$. The energy gap at the selected points is $E(\mathbf{p}_1) \approx 0.15\Delta$, $E(\mathbf{p}_2) \approx 0.063\Delta$, $E(\mathbf{p}_3) \approx 0.060\Delta$. (c) Similar diagram, but with $\xi/a = 2$, $R/a = 0.1$, The energy gap at the selected points is $E(\mathbf{p}_1) \approx 0.11\Delta$, $E(\mathbf{p}_2) \approx 0.15\Delta$, $E(\mathbf{p}_3) \approx 0.27\Delta$. (d) Square of wave-function amplitude $|\psi|^2$ for the lowest-lying positive energy wave function for a 25×25 lattice from the point $k_F a = 7.5$, $\eta = 1.6$ in (c).

and R is the radius of the magnet. Although small magnets pose a challenge to the fabrication process, in an experimental setting $k_F R \approx 1$ is already within reach since fabrication of nanomagnets with radius of a few tens of nanometers has become feasible [30]. With that in mind, in Fig. 2(a) we plot the bound-state energies as a function of R for selected system parameters. As seen in the figure, while for larger R the higher-l states get increasingly important, for our parameters around $k_F R = 1$, only the lowest few states are appreciably within the gap, and the very lowest is separated from the others by a finite energy, which raises hopes for the presence of robust topological phases in realistic parameter regimes. Hence, we expect that, for the studied parameter regime, a low value of $l_{\max} \lesssim 2$ should be an excellent approximation for the system with multiple magnets since the low-lying states are unlikely to couple strongly to those near the gap edge.

The validity of this assumption can be readily tested by examining the properties of a one-dimensional chain of magnets, which we have done in the SM [27]. We find that properties such as topology and energy gap at $l_{\max} = 1$ are essentially indistinguishable to those obtained for $l_{\max} = 2, \ldots, 7$ in the studied regime. Based on this, we conclude that, for the values of R and k_F used here, $l_{\max} = 1$ is already a good approximation of the system.

IV. TWO-DIMENSIONAL LATTICES

Now, we apply our theory to 2D systems. Guided by the single-magnet and 1D problems, we focus on the parameter regime where the angular momentum expansion can be cut at $l = 1$. Even with this truncation the nonlinear eigenvalue problem in Eq. (6) involves $12N \times 12N$ matrices, where N is the number of magnets. Working in k space would reduce the dimension to a 12×12 problem, but the relevant Fourier transforms cannot be carried out analytically. This fact, and the large number of bands, makes analytical work intractable even in k space. It is computationally more convenient to study the properties of finite systems in real space with periodic boundary conditions. In the considered parameter regime, finite-size properties converge rapidly even for relatively small systems.

To obtain the topological phase diagram, we must also evaluate the Chern number for the system. Typically, the calculation of the Chern number is formulated in momentum space, but it can be performed directly in real space. For this purpose, we will use the approach outlined in Ref. [31], requiring diagonalization of a real-space system with periodic boundary conditions, in a procedure briefly outlined in the SM [27]. In Figs. 2(b) and 2(c), we have plotted a topological phase diagram on a square lattice. As is seen in the figure, the selected parameter regimes support a wide range of topological phases, with Chern numbers varying from -15 to 9. Additional phases may be found by exploring other combinations of parameters. This abundance arises from the long-range intermagnet coupling terms in the system, following the arguments in Refs. [17,18]. The spectral problem can be solved numerically along the lines of Refs. [14,28], though the large number of orbitals and the 2D nature of the system makes the present case computationally demanding. We have calculated the energy gap at a few selected points from Figs. 2(b) and 2(c), listed in the figure caption. Notably, far from phase boundaries, systems in a nontrivial phase can have have energy gaps of the order of 0.25Δ or higher, which could optimally translate to temperatures $T \sim 1$ K. In general, the energy gap decreases as the Chern number increases. The Chern number of a 2D topological superconductor corresponds to the number of chiral edge modes around the system with open boundary conditions. The energies of the edge modes are located in the bulk excitation gap and provide an experimentally accessible fingerprint of the nontrivial topology. Indeed, as shown in Fig. 2(d), the states in the bulk gap of a nontrivial state are located on the edges of the sample.

It is important to address whether the parameter regime relevant to the system is feasibly achievable in experiment. As explained above, robust gapped states require that $k_F R \lesssim 1$, where R is the radius of the nanomagnet. Assuming that the radius of the nanomagnets is $R = 50$ nm, it follows that, for example, the other parameters in Fig. 2(c) are $\xi = 1\ \mu$m, $k_F \approx 2 \times 10^7\ \text{m}^{-1}$; the characteristic energy scale of magnetization in Figs. 2(b) and 2(c) is $M_i \sim 0.6$–1.2 meV. We compare this to two recent studies of InAs-based 2DEG-superconductor composite systems. References [32,33] employ the value $\Delta \approx 230\ \mu$eV. Using $m^* = 0.023 m_e$, $n_{2D} \approx 9 \times 10^{15}\ \text{m}^{-2}$ [32],

we obtain $k_F \approx 3.36 \times 10^8$ m^{-1}, $\xi \approx 3.4$ μm. Furthermore, from the spin-orbit energy $\frac{m^*\alpha^2}{2} = 118.5$ μeV [33] we obtain $\varsigma \approx 0.15$. We conclude that our parameters are approximately in line with those studied, provided that the electron density n_{2D} is reduced to $n_{2D} \approx 10^{14}$ m^{-2}. In 2DEG materials the Fermi level can be gated even down to zero, which is complicated here by the screening from the proximity superconductor. However, while adding a technical difficulty similar to some previous proposals, for example Ref. [5], the presence of a superconductor does not pose a fundamental obstacle for electrostatic control of density. The superconductor does not need to be in a direct contact with the whole magnetic area to induce a robust proximity gap. Modern fabrication technology allows even quite imaginative solutions such as creating a checkerboard pattern with alternating magnetic and superconducting regions [34]. The superconductivity may persist in proximity systems even for magnetic fields of several Teslas, so the system is expected to be robust against the local disruption due to the magnets.

V. DISCUSSION

There are two outstanding issues in the research of chiral topological superconductivity. The first one is the physical realization of chiral states in experimentally accessible systems, preferably in a way that allows a systematic study of states with distinct Chern numbers. The second one is to device a method that enables a unique identification of the Chern number of a state. Our work is a comprehensive effort toward the first goal. The second issue remains a challenge at the moment. The Majorana edge modes support a quantized thermal conductance determined by the number of modes which coincide with the Chern number. However, the required precision in the measurement of thermal transport is not feasible presently. While there exist proposals to identify the topological state through electric measurements [17,35], none of the known methods so far are general and practical enough to solve the problem satisfactorily. This is an area of active study and, due its versatility, the nanomagnet system is an excellent test bench for future proposals.

Aside from the rich topology, the key feature of the studied system comes from the significant tunability of the topological state. First of all, the structural control in the fabrication process enables controlling the lattice constant a and the geometry of the magnetic array. Different stacking will modify the topological state and allow a fabrication of multiple different topological domains in one sample with chiral Majorana edge channels separating them. More importantly, the state of the system is tunable by external control parameters after the fabrication. By tuning k_F by electronic gates and magnetization through external fields, it is possible to sample the different regions of the phase diagram in Figs. 2(b) and 2(c) *in the same system*. A realization of the studied system requires state-of-the-art experimental efforts, which is natural for the proposed highly ambitious goal.

VI. CONCLUSION

In this work, we have introduced a nanomagnet-semiconductor structure that serves as a universal platform for topological chiral superconductivity. This system supports several different topological states which can be tuned by structural design and electronic gates. The fabrication of the proposed system is within reach of current technology and could stimulate systematic research of mesoscopic superconductors with tunable Chern numbers in the near future.

ACKNOWLEDGMENTS

The authors would like to thank C. Marcus, S. Nadj-Perge, and P. Simon for discussions. This work is supported by the Academy of Finland and the Aalto Centre for Quantum Engineering. K.P. acknowledges the Finnish Cultural Foundation for financial support.

[1] C. Kallin and J. Berlinsky, Rep. Prog. Phys. **79**, 054502 (2016).
[2] G. E. Volovik, *The Universe in a Helium Droplet* (Oxford University Press, Oxford, UK, 2003).
[3] B. A. Bernevig and T. L. Hughes, *Topological Insulators and Superconductors* (Princeton University Press, Princeton, NJ, 2013).
[4] A. P. Schnyder, S. Ryu, A. Furusaki, and A. W. W. Ludwig, Phys. Rev. B **78**, 195125 (2008); S. Ryu, A. P. Schnyder, A. Furusaki, and A. W. W. Ludwig, New J. Phys. **12**, 065010 (2010).
[5] J. D. Sau, R. M. Lutchyn, S. Tewari, and S. Das Sarma, Phys. Rev. Lett. **104**, 040502 (2010).
[6] S. Nadj-Perge, I. K. Drozdov, J. Li, H. Chen, S. Jeon, J. Seo, A. H. MacDonald, B. Andrei Bernevig, and A. Yazdani, Science **346**, 602 (2014).
[7] M. Ruby, F. Pientka, Y. Peng, F. von Oppen, B. W. Heinrich, and K. J. Franke, Phys. Rev. Lett. **115**, 197204 (2015).
[8] T. P. Choy, J. M. Edge, A. R. Akhmerov, and C. W. J. Beenakker, Phys. Rev. B **84**, 195442 (2011).
[9] S. Nadj-Perge, I. K. Drozdov, B. A. Bernevig, and A. Yazdani, Phys. Rev. B **88**, 020407(R) (2013).
[10] B. Braunecker and P. Simon, Phys. Rev. Lett. **111**, 147202 (2013).
[11] J. Klinovaja, P. Stano, A. Yazdani, and D. Loss, Phys. Rev. Lett. **111**, 186805 (2013).
[12] M. M. Vazifeh and M. Franz, Phys. Rev. Lett. **111**, 206802 (2013).
[13] F. Pientka, L. I. Glazman, and F. von Oppen, Phys. Rev. B **88**, 155420 (2013).
[14] K. Pöyhönen, A. Westström, J. Röntynen, and T. Ojanen, Phys. Rev. B **89**, 115109 (2014).
[15] A. Heimes, P. Kotetes, and G. Schön, Phys. Rev. B **90**, 060507(R) (2014).
[16] P. M. R. Brydon, S. Das Sarma, H.-Y. Hui, and J. D. Sau, Phys. Rev. B **91**, 064505 (2015).
[17] J. Röntynen and T. Ojanen, Phys. Rev. Lett. **114**, 236803 (2015).
[18] J. Röntynen and T. Ojanen, Phys. Rev. B **93**, 094521 (2016).

[19] J. Li, T. Neupert, Z. J. Wang, A. H. MacDonald, A. Yazdani, and B. A. Bernevig, Nat. Commun. **7**, 12297 (2016).
[20] G. C. Ménard *et al.*, Nat. Phys. **11**, 1013 (2015).
[21] L. Yu, Acta Phys. Sin. **21**, 75 (1965).
[22] H. Shiba, Prog. Theor. Phys. **40**, 435 (1968).
[23] A. I. Rusinov, Zh. Eksp. Teor. Fiz., Pis'ma v Redaktsiyu **9**, 146 (1969) [JETP Lett. **9**, 85 (1969)].
[24] A. V. Balatsky, I. Vekhter, and J.-X. Zhu, Rev. Mod. Phys. **78**, 373 (2006).
[25] Y. Kim, J. Zhang, E. Rossi, and R. M. Lutchyn, Phys. Rev. Lett. **114**, 236804 (2015).
[26] J. Zhang, Y. Kim, E. Rossi, and R. M. Lutchyn, Phys. Rev. B **93**, 024507 (2016).
[27] See Supplemental Material at http://link.aps.org/supplemental/10.1103/PhysRevB.96.174521 for details on the derivations of the results in the main text, and a treatment of the special-case scenario of a 1D chain.
[28] A. Weststrom, K. Pöyhönen, and T. Ojanen, Phys. Rev. B **91**, 064502 (2015).
[29] K. Pöyhönen, A. Weststrom, and T. Ojanen, Phys. Rev. B **93**, 014517 (2016).
[30] G. C. Ménard, S. Guissart, C. Brun, M. Trif, F. Debontridder, R. T. Leriche, D. Demaille, D. Roditchev, P. Simon, and T. Cren, arXiv:1607.06353.
[31] Y. F. Zhang, Y. Y. Yang, Y. Ju, L. Sheng, D. N. Sheng, R. Shen, and D. Y. Xing, Chin. Phys. B **22**, 117312 (2013).
[32] J. S. Lee, B. Shojaei, M. Pendharkar, A. P. McFadden, Y. Kim, H. J. Suominen, M. Kjaergaard, F. Nichele, C. M. Marcus, and C. J. Palmstrøm, arXiv:1705.05049.
[33] M. Hell, M. Leijnse, and K. Flensberg, Phys. Rev. Lett. **118**, 107701 (2017).
[34] C. Marcus (private communication).
[35] S. Rachel, E. Mascot, S. Cocklin, M. Vojta, and D. K. Morr, arXiv:1705.05378.